

## The Role of the Gulf of California in the North American Monsoon

BENJAMIN O. JOHNSON<sup>a</sup> AND THOMAS L. DELWORTH<sup>b</sup>

<sup>a</sup> Program in Atmospheric and Ocean Sciences, Princeton University, Princeton, New Jersey

<sup>b</sup> NOAA/Geophysical Fluid Dynamics Laboratory, Princeton, New Jersey

(Manuscript received 13 May 2022, in final form 2 October 2022)

**ABSTRACT:** The role of the Gulf of California (GoC) in the North American monsoon (NAM) is investigated using a global climate model with 50-km horizontal atmospheric resolution and prescribed SSTs. Specifically, two 135-yr simulations are compared to quantify the influence of the GoC on the NAM: in the first simulation a realistic representation of the GoC is incorporated, while in the second simulation the GoC is replaced with land surface. The results suggest that the GoC has a significant impact on circulation, with cooler surface air temperatures and lower surface friction allowing for south-southeasterly surface flow along the entire length of the GoC, in turn increasing low-level moisture fluxes into the NAM region. Cooler air over the GoC also leads to lower heights at 700–500 hPa, with a corresponding cyclonic moisture flux anomaly, further increasing moisture fluxes into the NAM region. Correspondingly, precipitation is substantially higher over the NAM region and even east of the Continental Divide in areas such as New Mexico and the U.S. Great Plains. July/August precipitation with a realistic GoC is generally 25%–50% greater in northwestern Mexico than the land-filled case, with precipitation 50% greater in much of the southwestern United States. Due to enhanced surface evaporation, areas with increased precipitation also tend to have lower surface temperatures, higher sea level pressure, and lower mid- to upper-tropospheric heights, thus altering the large-scale circulation. These results highlight the importance of the GoC in the NAM and demonstrate the necessity of resolving the GoC in climate simulations.

**SIGNIFICANCE STATEMENT:** This paper seeks to improve our understanding of the North American monsoon, an important moisture source in the relatively arid region of northwest Mexico and the Southwest United States. Specifically, we investigate the role of the Gulf of California: a long, narrow sea surrounded by elevated topography within the North American monsoon region, oriented roughly southeast–northwest. The results suggest the Gulf of California is an important component of the North American monsoon system. We find that the Gulf of California acts to enhance moisture transports into the North American monsoon, leading to substantially higher precipitation over a large region. Therefore, the Gulf of California should be carefully considered in climate simulations and future projections, especially given it is often not well resolved.

**KEYWORDS:** Atmosphere; North America; Atmosphere-ocean interaction; Hydrologic cycle

### 1. Introduction

#### *a. Overview of the NAM system*

The North American monsoon (NAM) is a distinct warm-season atmospheric circulation regime over northern Mexico and the southwestern United States (SWUS) that results in a summertime (June–September, but most predominant in July/August) peak in rainfall in those regions (e.g., Douglas et al. 1993; Adams and Comrie 1997). In a general sense, precipitation during the NAM results from the seasonal northward migration of maximum solar radiation. This causes westerlies, which would otherwise advect stable air from the relatively cool Pacific (see July/August mean SSTs in Fig. 1) into the region, to weaken and shift northward (Barlow et al. 1998). Meanwhile, seasonally intense, elevated solar insolation over northern Mexico and the southwestern U.S., and the westward expansion of the Bermuda high, draw in moist air from the south and southeast, setting the stage for deep convection to occur. In the NAM region (northwestern Mexico

and the SWUS), the lower troposphere is divided by high north–south topography (Fig. 1). Low-level moisture east of the Continental Divide is primarily sourced from the Atlantic basin, while low-level moisture west of the Continental Divide is primarily from the GoC and eastern Pacific (Jana et al. 2018; Dominguez et al. 2016). In the middle troposphere, where air is not directly blocked by the Continental Divide, southeasterly flow of moist air from the Atlantic side along the western flank of the Bermuda high is important at both sides of the Continental Divide.

The NAM onset occurs rapidly during June in the western slopes of the Sierra Madre Occidental in northwest Mexico, typically continuing to extend farther northwest into the SWUS in early July (Barlow et al. 1998; Higgins et al. 1999). The heaviest rainfall associated with the NAM occurs in the western foothills of the Sierra Madre Occidental. Significant NAM-related precipitation, albeit less impressive, extends into the SWUS, and intermittently stretches as far north as the Idaho–Utah border and into Wyoming, and is generally most intense in the higher terrain (Adams and Comrie 1997). Reanalysis and station-based data suggest that as much as 30% to +40% of annual precipitation occurs during July/August in Arizona/New Mexico, and widespread amounts of

Corresponding author: Benjamin O. Johnson, boj2@princeton.edu

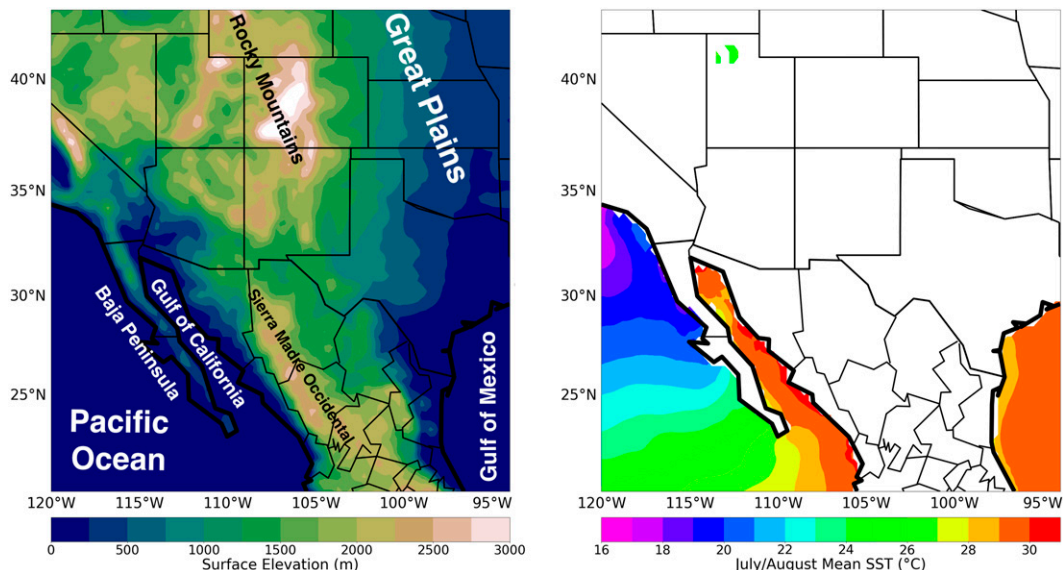


FIG. 1. (left) ERA5 (Hersbach et al. 2020) surface elevation and major geographic features. (right) ERA5 1979–2020 July/August mean SSTs.

40% to 50%+ of annual precipitation in northwestern Mexico (Fig. 2). The NAM influence extends beyond its peak in the months of July and August, and therefore the true percentage of annual precipitation related to the NAM is even higher. Thus, the NAM is an important hydroclimate system.

The NAM is a relatively poorly understood hydroclimate system and has proven a challenge to prediction systems (Castro et al. 2012). Additionally, global climate models show qualitative disagreement in projecting the response of the NAM to future changes in radiative forcing from greenhouse gases and aerosols (Cook and Seager 2013; Meyer and Jin 2017; Pascale

et al. 2017), whereas models tend to suggest a robust intensification of other global monsoons due to greater atmospheric water vapor content (Hsu et al. 2012; Kitoh et al. 2013; Lee and Wang 2014). An improved dynamical understanding of the NAM system can potentially improve seasonal predictions and future projections.

#### b. Large-scale dynamics of the NAM

Although the NAM is not directly related to the seasonal shift in the intertropical convergence zone (ITCZ) as is more

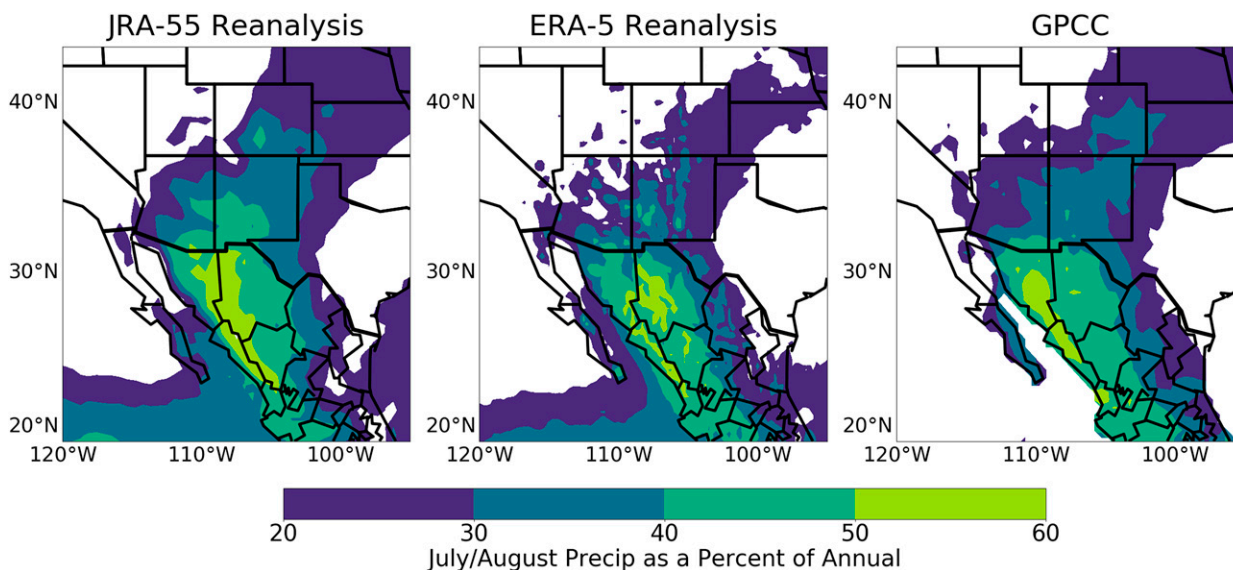


FIG. 2. Percent of annual precipitation occurring during the months of July and August for the period 1979–2020 as estimated by the (left) JRA55 (Japan Meteorological Agency 2013), (center) ERA5 (Hersbach et al. 2020), and (right) station-based Global Precipitation Climatology Center (GPCC; Schneider et al. 2011).

clearly apparent in other global monsoon systems (e.g., Gadgil 2018), the NAM displays robust monsoon-like circulation features. At 500 hPa, relatively dry southwesterly flow in northwestern Mexico and the SWUS in early June transitions into an east-southeasterly regime associated with the seasonal westward expansion of the subtropical Atlantic surface anticyclone by July (Adams and Comrie 1997), with a tongue of moist air extending from the Gulf of Mexico across the NAM region and northeastward into the Great Plains in the middle troposphere. The seasonal westward expansion of the Bermuda high is also related to the formation of the Great Plains low-level jet (Zhu and Liang 2013), though moisture is limited to the middle levels west of the Continental Divide due to the blocking effect of the high topography (e.g., Dominguez et al. 2016; Jana et al. 2018).

Intense elevated solar heating over western North America and Mexico is another driver of the NAM (Tang and Reiter 1984). While often compared to the effect of elevated heating of the Tibetan Plateau, as is the case in Tang and Reiter (1984), Boos and Kuang (2010) bring some doubt to the role of the Tibetan Plateau's elevated heating in the south Asian monsoon. Their idealized topography–heating model experiments suggest the Tibetan Plateau's elevated heating plays a secondary role to the Himalayas, which act as a topographic barrier, preventing the intrusion of cooler, drier air from the north. However, in the NAM, relative maximum 850-hPa temperatures occur in the SWUS, coinciding with the strong, elevated solar insolation, and an east–west cross section of July vertical velocity shows a clear pattern of ascent over elevated topography and descent over adjacent non-elevated areas (Barlow et al. 1998). This suggests a more direct role of elevated heating in the NAM. Boos and Pascale (2021), however, emphasize the role of mechanical rather than thermal forcing of NAM topography. For example, in one experiment, they flatten Mexican topography, and in an additional experiment lower the albedo of a flattened Mexico to explore the role of thermal forcing. They find the flattening topography in Mexico has a much larger effect than decreasing the albedo (i.e., increasing surface net radiation) of a flattened Mexico. However, with no topographic barrier, one might expect ventilation of cool, stable Pacific air to severely inhibit deep convection. For example, Pascale et al. (2016) and Varuolo-Clarke et al. (2019) explore the impact of model resolution on simulated NAM characteristics, and point to a diminished topographic barrier at lower resolutions, particularly a somewhat flattened Baja Peninsula, as a cause for NAM simulation degradation at lower resolution. This is a parallel to the results of Boos and Kuang (2010), in that the California/Baja Peninsula topography may play a similar role to the Himalayas in blocking cooler, drier air from ventilating the monsoon (and thus suppressing precipitation). On this note, it would be interesting to explore the sensitivity of a simulated NAM to changes in the albedo imposed on the region's elevated topography. Nevertheless, elevated heating does appear to play a crucial role in the NAM system, though future work and debate on this subject is certainly warranted.

Similar to other monsoon systems, an anticyclone with accompanying outflow is present in the upper troposphere in

northwest Mexico and the SWUS. The anticyclonic shear line at the northern boundary of the monsoon anticyclone coincides with the northern edge of NAM precipitation near the Utah–Idaho border and eastward into Wyoming (Tang and Reiter 1984). Interestingly, the observed early-summer decrease in Great Plains precipitation tends to coincide with the onset of the NAM. This occurs despite ever-strong moisture transports by the Great Plains low-level jet and appears to result from induced 200-hPa convergence north and east of the monsoon high in the western United States (Higgins et al. 1997). The fact that vertical ascent is strong in the month of June before the NAM onset, (in fact, 500-hPa ascent over the Southwest United States is likely greater prior to NAM onset; Higgins et al. 1997), suggests there may be a role of NAM deep convective heating in establishing the upper-tropospheric anticyclone and thus suppressing rainfall in the Great Plains.

### c. NAM moisture sources and the importance of the GoC

An important NAM feature is the presence of low-level south-southeasterly flow in the GoC (Douglas 1995), which acts to supply low-level moisture west of the Continental Divide. This pattern is related to the land–sea thermal contrast driven by the strong elevated heating. Near the surface, heat lows, strongest in the low desert terrain north of the GoC, extend to 700 hPa (Rowson and Colucci 1992). The low sea level pressure acts to draw anomalous low-level moisture into the NAM region compared to before the onset of NAM rainfall: a sea level pressure gradient forms along the GoC axis, with climatological low-level south-southeasterly flow along the GoC toward the heat low, in contrast to the northwesterly flow dominating preseason (Bordoni et al. 2004). The sea level pressure gradient along the GoC is correlated at the 99% level of significance with the 1000–500-hPa thickness between the NAM anticyclone centered over northwestern Mexico and that south of the GoC (Turrent and Cavazos 2009). Stronger, earlier NAM onsets tend to occur in years with unusually strong land–sea contrast just prior to onset. However, the relationship is complicated due to land feedbacks (greater precipitation tends to result in surface cooling via increased surface evaporation, which acts to weaken the land–sea contrast).

The GoC low-level flow, though south-southeasterly in the mean and with a low-level nocturnal jet present on the majority of monsoon days (Douglas 1995), varies throughout the NAM season. Periods of stronger, deeper southerly flow, known as “surge” events, typically occur intermittently throughout the season, often with anomalously heavy rainfall (Hales 1972; Brenner 1973). Surge events are generally triggered by the passage of tropical easterly waves to the south of the GoC, passing tropical cyclones, or convective outflow during weaker surge events (e.g., Zehnder 2004).

As discussed, due to the high north–south topography, moisture east of the Continental Divide is mainly of easterly origin, such as from the Gulf of Mexico, whereas moisture west of the Continental Divide mainly comes from the GoC and eastern Pacific (Jana et al. 2018). Precipitation recycling is also important, with model studies suggesting land evapotranspiration

has a significant contribution to precipitation (Dominguez et al. 2016; Jana et al. 2018; Ordoñez et al. 2019). Although both low-level and midlevel moisture contribute significantly to NAM precipitation, low-level moisture is more abundant and of special importance due to its destabilizing effect. NAM precipitation is largely a function of convective available potential energy (CAPE), a measure of air parcel buoyancy potential when lifted (Adams and Souza 2009). All else equal, greater low-level moisture leads to increased CAPE via stronger latent heating during moist adiabatic ascent. For this reason, southerly moisture fluxes through the GoC are a crucial feature of the NAM west of the Continental Divide. Indeed, the Dominguez et al. (2016) model study suggests moisture from the GoC is converted to precipitation more efficiently than that from other sources due to its role in establishing positive CAPE. In fact, an estimated 70% of NAM season precipitation in Arizona occurs during days of enhanced southerly flow in the GoC (Becker and Berbery 2008).

Despite the emphasized importance of low-level moisture from the GoC west of the Continental Divide, easterly moisture fluxes play a significant role in the NAM. This is especially true east of the Continental Divide (e.g., New Mexico) where the majority of moisture originates from easterly sources (e.g., the Gulf of Mexico; Jana et al. 2018). Although this easterly moisture is blocked by high north–south-oriented topography west of the Continental Divide (Jana et al. 2018; Dominguez et al. 2016), observational evidence suggests that, despite being limited to the mid- to upper levels, this moisture contributes to precipitation. For example, enhanced easterly moisture fluxes have been identified as a distinguishing factor allowing for surge events with heavier rainfall in the SWUS and related to SWUS summer precipitation anomalies (Schiffer and Nesbitt 2012; Ordoñez et al. 2019). Thus, despite the special importance of low-level moisture entering the NAM region through the GoC, the nature of moisture fluxes in the NAM and their importance for precipitation remains a complex picture. The question of how much the observed intensity and extent of the NAM depends on the existence of the GoC is a focal point this study explores.

The goal of this study is to better understand dynamic processes occurring over the GoC, and how important they are in driving the observed NAM precipitation. This has been the topic of several previous works. Multiple studies have noted that low-resolution models are unable to resolve circulation features over the GoC, including the low-level mean south-southeasterly flow and stronger surge events, highlighting the importance of the channel-like topography surrounding the GoC (Pascale et al. 2016; Varuolo-Clarke et al. 2019). Specifically, the Baja Peninsula acts to largely block the influence of stable Pacific air, with tropical air funneling into the NAM region through the topographic channel in which the GoC lies. The GoC sea surface may be important, in addition to the channel-like topography, as is explored in this study. The GoC sea surface could have two effects: altering the atmospheric circulation via altered lower-tropospheric temperature gradients and reduced surface friction, and supplying moisture directly via surface evaporation over its relatively warm waters.

Interestingly, GoC sea surface temperatures imposed in a climate model that are more characteristic of the adjacent Pacific drastically reduced NAM precipitation (Stensrud et al. 1995), and observations suggest that NAM rainfall migrates north with the migration of warm GoC SSTs (Mitchell et al. 2002). While one might expect GoC SST isotherms to progress with NAM onset given both are related to the seasonal increase in solar radiation, the NAM onset migrates in suspiciously close correspondence with the 29.5°C GoC SST isotherm. Erfani and Mitchell (2014) suggest the apparent synchronous progression of GoC isotherms and the NAM onset relates to changes in the boundary layer over the GoC as SSTs warm. If GoC SSTs are too cold, a steep temperature inversion confines moisture to a narrow layer near the surface. Erfani and Mitchell (2014) suggest the 29.5°C isotherm is sufficient to substantially erode the temperature inversion over the GoC, allowing for a much deeper influx of moisture, and thus the onset of the NAM. This would explain the high sensitivity of simulated NAM precipitation to low GoC SSTs found in Stensrud et al. (1995). Increased surface evaporation from the GoC due to warmer SSTs and the mixing of drier air from aloft with a weakened inversion may also play a role in this apparent sensitivity of NAM rainfall to GoC SSTs. Model tracer studies suggest moisture from GoC surface evaporation contributes significantly to NAM precipitation (Dominguez et al. 2016; Jana et al. 2018). Given these factors, one might expect more NAM precipitation with higher GoC SSTs imposed in models. However, model studies imposing anomalously warm GoC sea surface temperatures find the positive effect of GoC SSTs on rainfall is apparent yet limited due to unfavorable effects of warmer SSTs on moisture fluxes related to a decreased land–sea thermal contrast (Mo and Juang 2003; Kim et al. 2005). It could be the case that there is a sharp positive effect of increasing GoC SSTs on NAM rainfall near 29.5°C, with relatively small changes beyond that threshold. However, the lack of response in these model studies could potentially stem from unrealistic modeled GoC boundary layer dynamics.

In this study, we isolate the effect of the GoC in the NAM. In other words, how would the NAM system respond if the GoC were instead land surface? By exploring the effect of the GoC, the aim is to provide a missing piece to the puzzle of understanding the GoC dynamic regime. Furthermore, many climate models do not accurately resolve the GoC sea surface, and it is important to understand the effect this has on the simulated NAM. Finally, we hope to provide an interesting case study of how the larger-scale NAM and surrounding climate respond to more localized, direct changes in atmospheric circulation and moisture fluxes over the GoC.

## 2. Methods

### a. Model setup

The goal of this study is to assess to the role of the GoC in the NAM. To accomplish this goal, we run two simulations with altered land–sea boundaries in the GoC: one with a realistic, water-filled GoC (hereon referred to as GoC\_WATER),

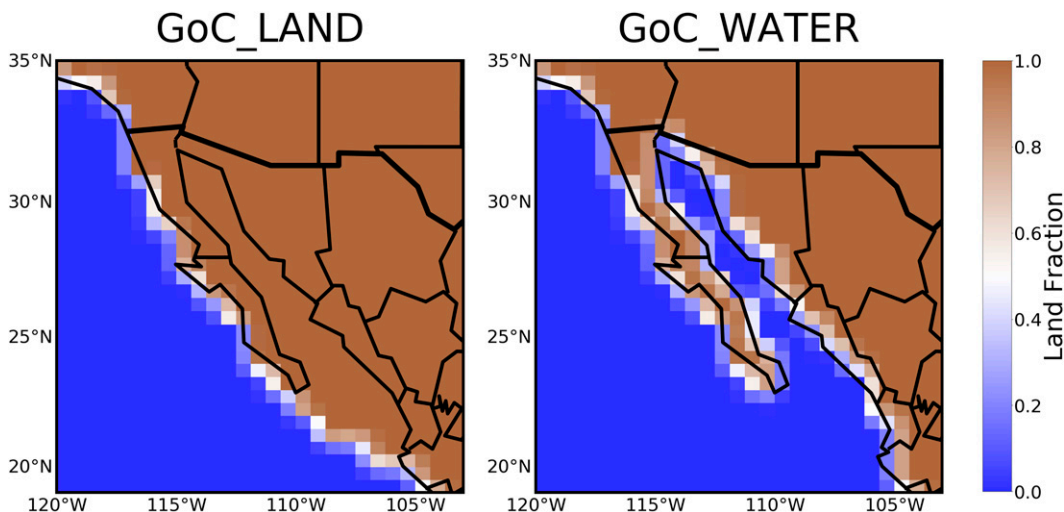


FIG. 3. Land masks used for simulations. Values represent the fraction of a grid box that is covered with land (grid boxes along coastlines may contain both land and ocean).

and one where the GoC is instead represented as flat land surface (hereon referred to as GoC\_LAND). By taking the difference between these simulations (GoC\_WATER minus GoC\_LAND), we can quantify the effect of the GoC on the NAM in the model, and use that as an estimate of the role of the GoC in the real-world NAM.

We use a model called Seamless System for Prediction and Earth System Research (SPEAR; Delworth et al. 2020) to perform our simulations. SPEAR is a Geophysical Fluid Dynamics Laboratory (GFDL) global climate model designed for seasonal to multidecadal predictions and projections. The atmospheric component of the model is very similar to the CM4 atmospheric model (Held et al. 2019) with 33 atmospheric levels. The land component is nearly identical to LM4 (Zhao et al. 2018). The boundary layer scheme used is described in Lock et al. (2000).

An important factor of consideration in the experimental setup is the horizontal atmospheric resolution. Models with low atmospheric resolution fail to resolve GoC processes (Pascale et al. 2016; Varuolo-Clarke et al. 2019). Pascale et al. (2016) found a substantial increase in model performance for a resolution increase from 200 to 50 km, with a relatively small increase upon further increasing resolution to 25 km. To balance resolution and computational efficiency, the 50-km atmospheric resolution version of SPEAR is used. Sea surface temperature biases are another important factor to consider in NAM simulations. For example, biases in the Atlantic often lead to a delayed retreat of the NAM (Liang et al. 2008; Geil et al. 2013; Pascale et al. 2017). To account for this, and to further limit the potential for internal variability that may obscure results, climatological SSTs are imposed instead of using the fully coupled version. SSTs are derived from the Hadley Centre Ice and Sea Surface Temperature dataset ( $1^\circ \times 1^\circ$  resolution; Rayner et al. 2003), except in the northern portion of the GoC due to a cold bias resulting from the intrusion of cooler Pacific SSTs in the model's interpolation scheme (the model interpolates the data over all grid points in

order to assign values to narrow water bodies such as the GoC). Here, we use higher resolution ERA5 1979–2020 SSTs ( $0.25^\circ \times 0.25^\circ$  resolution; Hersbach et al. 2020), changing SSTs to that of the nearest GoC grid box in areas not covered by the dataset (ERA5 SSTs are only used in this area in order to be consistent with available SPEAR climatological SST experiments). This is especially important as overly cool SSTs in the GoC can substantially limit simulated NAM precipitation (Stensrud et al. 1995).

The land–sea boundaries used in our simulations are shown in Fig. 3. In GoC\_LAND, the entire GoC and water directly southeast are converted to land. The idea behind converting this additional area southeast of the traditional GoC to land is to have a smooth coastline. However, this area could be left as water in a similar future study. In SPEAR, each atmospheric grid box has one or more surface types (or multiple ocean surfaces each tied to an ocean grid box overlying a portion of the atmospheric grid box). Each surface occupies a fraction (0–1) of the grid box. Surface fluxes are computed for each surface individually, then the total flux with respect to the atmospheric grid box is computed by weighing each surface flux based on the fraction of the cell each surface occupies. Thus, assuming SSTs are sufficiently warm and the land is relatively dry, as is the case in the GoC, mean surface evaporation will generally increase as the land fraction decreases.

When changing water to land in the model, land properties must be set. Each land cell (corresponding to the same grid as the atmospheric component) has various properties. Caution is required as the land properties affect the atmospheric component of the model. For example, differences in surface friction and surface albedo can alter the atmospheric momentum and energy balance. Most of the grid points converted to land already have assigned land properties due to having a partial land fraction in the default version of SPEAR, but land properties must be assigned for grid boxes with an initial land fraction of zero. To do this, we assign land properties of the nearest grid box. Nearly all grid points in the traditional GoC

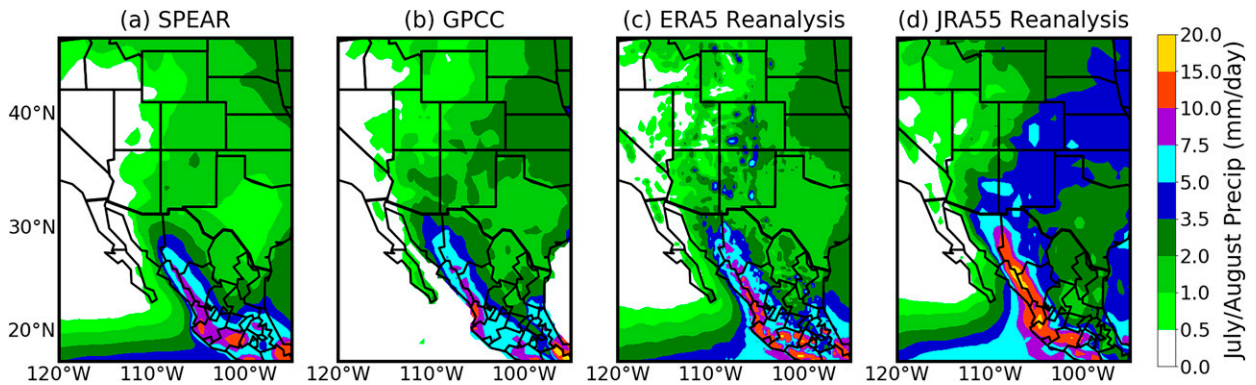


FIG. 4. July/August mean precipitation. (a) SPEAR, (b) GPCC 1979–2020, (c) ERA5, and (d) JRA55 1979–2020.

already have assigned land properties, but many grid points farther southeast must be assigned land properties in this way. To ensure that the GoC is fully represented as land, and not as swampy terrain that could act as a strong moisture source, rivers are turned off in the new land grid points. Simulations are run using preindustrial (1850) forcing for 135 years each to allow sufficient time for a clear signal to arise.

#### b. SPEAR NAM performance

To evaluate SPEAR's ability to simulate NAM features, July/August climate variable means are compared with the ERA5 (Hersbach et al. 2020) and JRA55 (Japan Meteorological Agency 2013) datasets, and the Gridded Precipitation Climatological Centre (GPCC) station-based precipitation dataset (Schneider et al. 2011). The GoC\_WATER experiment is used for comparison as this is the most realistic GoC configuration.

Precipitation comparisons are shown in Fig. 4. The general shape of NAM precipitation is in agreement between SPEAR and all three datasets, including the core of heaviest precipitation in the western Sierra Madre slopes of northwestern Mexico just east of the GoC, the rapid decline westward, as well as some of the locally higher precipitation in the elevated terrain of the SWUS. However, SPEAR has a significant dry bias in comparison to all three datasets over most of the region, especially in far northwestern Mexico and the SWUS.

SPEAR replicates important regional sea level pressure features including the high pressure off the California coast, low pressure in the SWUS, and higher sea level pressure eastward toward the Gulf of Mexico and Great Plains region of the United States (Figs. 5a–c). Accordingly, SPEAR simulates the mean surface south-southeasterly flow over the GoC and into the NAM region, and Great Plains low-level jet. 500-hPa heights (Figs. 5d–f) are in good qualitative agreement, with a maximum height located near the U.S.–Mexico border. However, 500-hPa heights in SPEAR are too high and centered a bit too far northwest in comparison, which may relate to higher surface temperatures caused by the dry bias (which increases the sensible to latent heat ratio). Column-integrated moisture fluxes and water vapor (Figs. 5g–i) are in good qualitative agreement between SPEAR and the reanalyses, including the tongue of southeasterly integrated moisture flux and relatively higher atmospheric moisture content stretching

northwest through the GoC and into the SWUS. Once again, there is a dry bias in terms of total column water vapor in spite of qualitative agreement. The dry bias could be related in part to the nearly pure easterly 500-hPa mean winds in the southern GoC in SPEAR, whereas the reanalyses show a poleward component (Figs. 5d–f). While there is an overall dry bias in SPEAR, the model is able to reproduce the overall structure of the NAM system.

### 3. Results

#### a. Surface circulation

July/August mean surface winds for each simulation are shown in Fig. 6. The GoC has a large impact on surface circulation over its boundaries in SPEAR, with a clear difference in direction of surface winds over the GoC between GoC\_WATER and GoC\_LAND, especially in the northern GoC. In GoC\_LAND, July/August mean surface winds over the northern GoC are westerly and represent an intrusion of cooler, stable Pacific air, whereas a south-southeasterly flow parallel to the GoC arises in GoC\_WATER. Correspondingly, GoC\_LAND has a much stronger sea level pressure gradient along the Baja Peninsula and southern GoC than GoC\_WATER. Cooler surface air temperatures, resulting from the cooler GoC sea surface, are primarily responsible for the robust increase in sea level pressure. This is evidenced in Fig. 7, where it is seen that the higher sea level pressures in GoC\_WATER very closely match the surface air temperature changes. In GoC\_WATER, surface air temperatures are 5°–10°C cooler over the GoC, with sea level pressure increases greatest in the northern GoC where they are more than 2 hPa higher than in GoC\_LAND. The local minimum sea level pressure in the Sonoran desert is lower in GoC\_LAND, but the sea level pressure gradient is more evenly distributed along the GoC in GoC\_WATER, equating to a stronger southeast–northwest gradient in the northern GoC and weaker gradient from the Pacific along the Baja Peninsula. This change allows for south-southeasterly mean flow to be present in the northern GoC, with less intrusion of cool Pacific air. Thus, the GoC alters the thermally driven surface circulation in a way favorable to supplying moisture to the NAM region. It has previously been noted that the thermal contrast between the Pacific

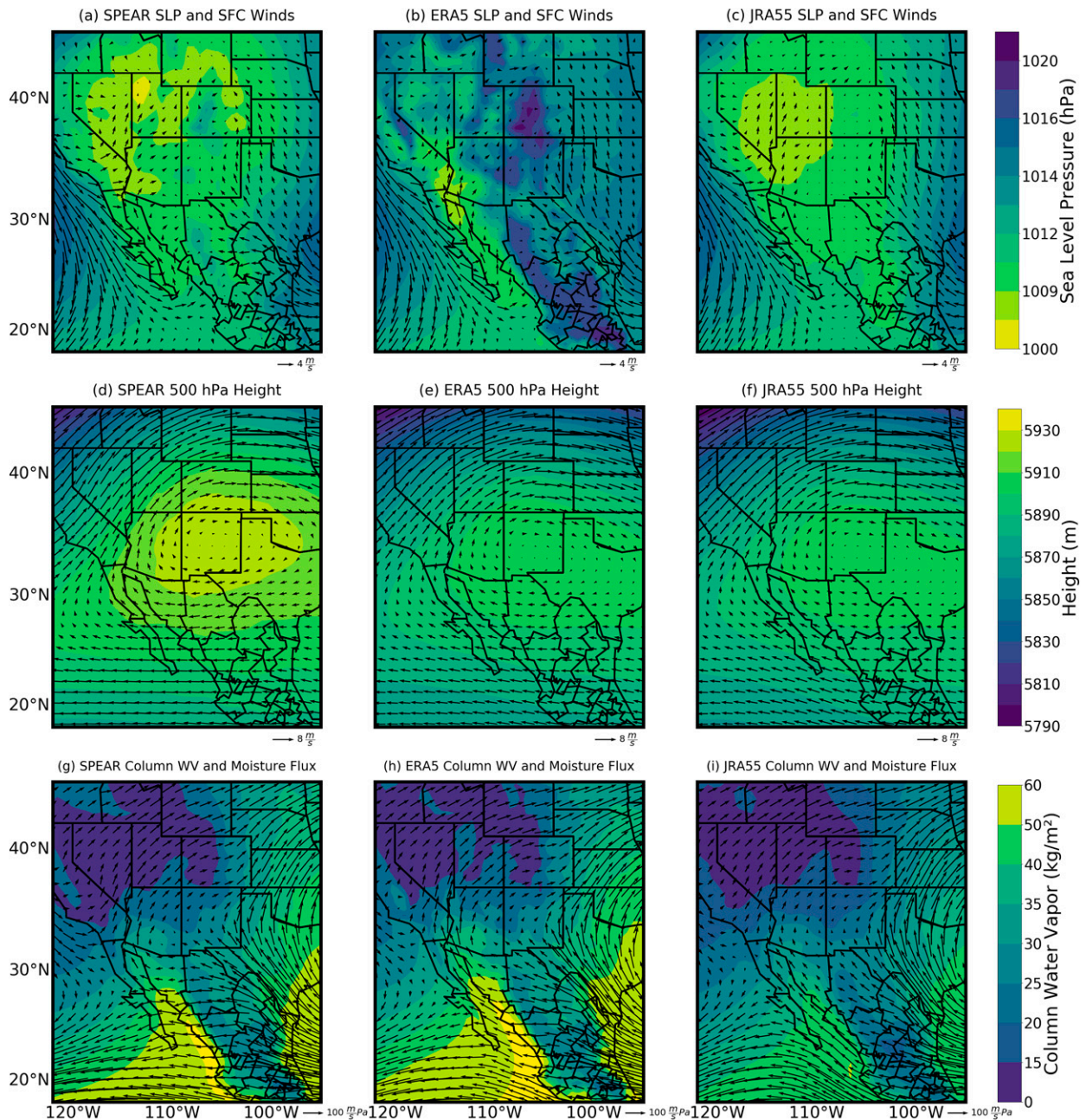


FIG. 5. (left) SPEAR (GoC\_WATER), (center) ERA5 1979–2020, and (right) JRA55 1979–2020 July/August variable means. Each row represents comparisons for the July/August means of different variables: (a)–(c) sea level pressure, (d)–(f) 500-hPa height, and (g)–(i) column-integrated water vapor and column-integrated moisture flux.

and GoC helps set up favorable moisture fluxes (Carleton et al. 1990), though our results suggest there may be an optimal balance between having a sea level pressure gradient strong enough to allow for southerly flow through the GoC, but not so strong that significant cool, stable air intrudes from the Pacific farther north.

The emergence of southeasterly flow in the GoC in GoC\_WATER is also partially attributable to the lower surface friction of water than land. This is especially apparent in the

southern GoC, where there is a strengthening of south-southeasterly winds despite a weaker sea level pressure gradient (Fig. 7a). Accordingly, the change in surface drag in the southern GoC is in the opposite direction as the change of surface winds in GoC\_WATER (Fig. 7b), consistent with the reduced surface friction. If not for the lower surface friction, surface wind anomalies in GoC\_WATER would tend to diverge from the maximum sea level pressure anomaly in the north-central GoC. In effect, although GoC winds would

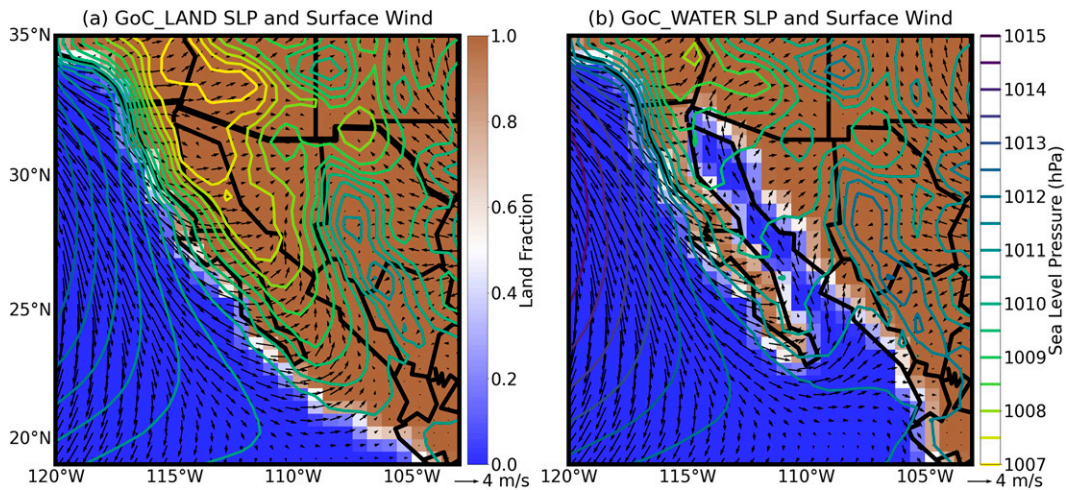


FIG. 6. Land masks (shading), surface winds (vectors), and sea level pressure (contours) for (a) GoC\_LAND and (b) GoC\_WATER. July/August means.

likely still be south-southeasterly along the entire axis owing to the sea level pressure gradient along its axis (Fig. 6), they would not be as robust. Further simulations isolating the influence of land versus sea surface friction and surface temperature changes would help assess the specific impact of thermal and frictional changes. Nonetheless, both factors appear important in allowing for south-southeasterly surface wind to prevail along the GoC in GoC\_WATER.

#### b. Circulation changes above surface

Circulation changes over the GoC extend above the surface. At 925 hPa, an anticyclonic circulation anomaly is apparent in GoC\_WATER in correspondence with higher heights (Fig. 8). The increased height is related to the aforementioned surface cooling-driven increase in sea level pressure. The higher heights are centered in the northern GoC, but extend over a larger region than the sea level pressure increases. Although the effects of

topography are still visible at this level, with winds somewhat warped toward the shape of the channel-like topographic feature in which the GoC sits, we do not see the increased south-southeasterly flow in the southern GoC as is apparent at the surface (Fig. 6). This is potentially due to the limited impact of changes in surface friction at this level. Geopotential height anomalies in GoC\_WATER change sign by 700 hPa. At this level, heights are a few meters lower in GoC\_WATER, with anomalies centered in the north-central GoC. This allows for southerly flow east of the GoC. By 500 hPa, low height anomalies in GoC\_WATER extend over a much broader area northeast of the GoC, due in part to larger scale land feedbacks related to precipitation changes (to be discussed).

#### c. Moisture fluxes and specific humidity

The GoC has a significant influence on moisture fluxes in both the lower and middle troposphere in our simulations. In

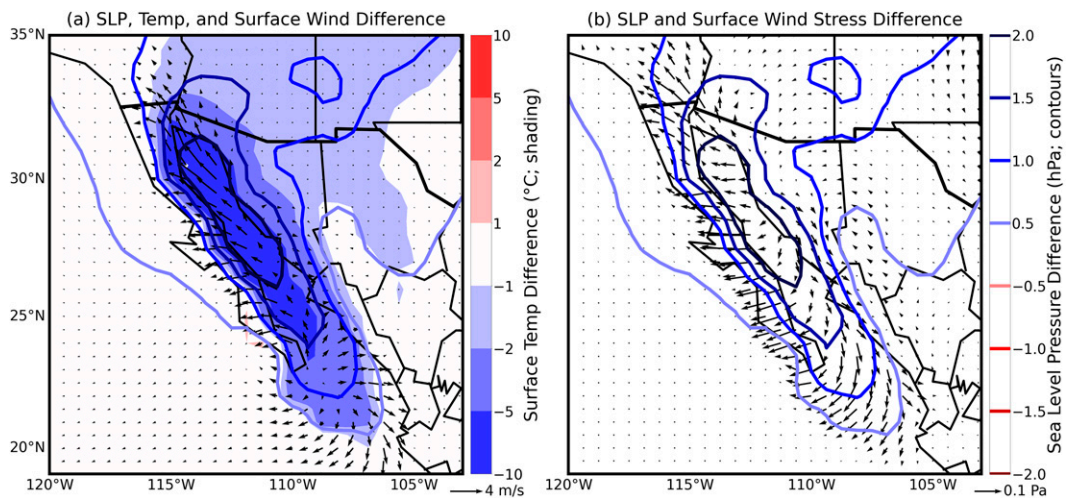


FIG. 7. July/August differences (GoC\_WATER – GoC\_LAND) in sea level pressure (contours in both panels): (a) surface winds (vectors) and (b) surface friction drag (vectors).

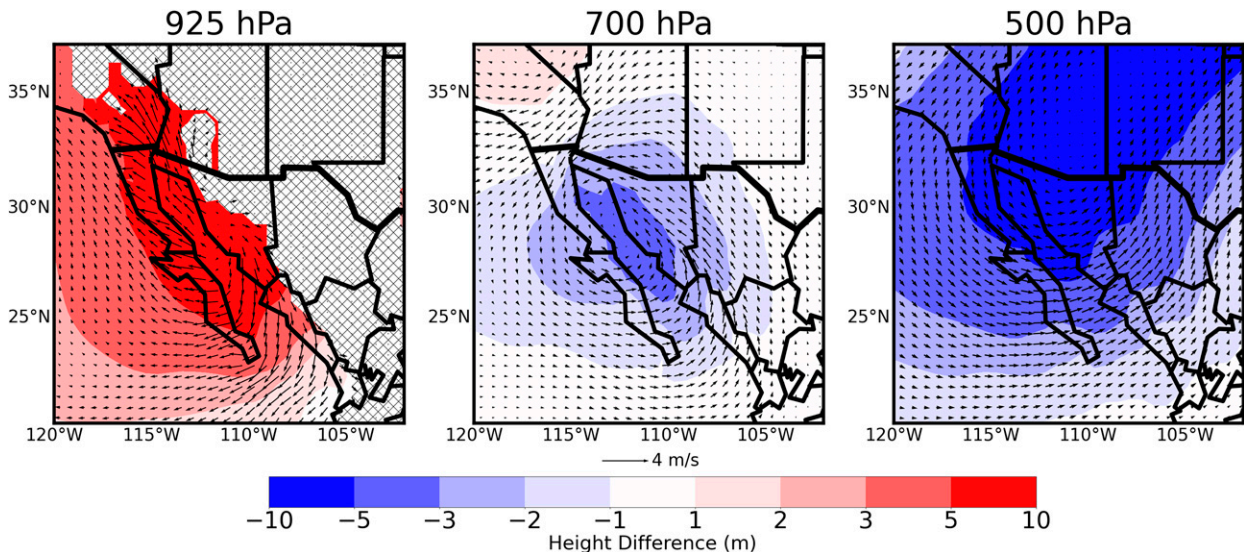


FIG. 8. July/August mean differences (GoC\_WATER – GoC\_LAND) in geopotential height (shading) and winds (vectors) for the GoC region. Areas where the surface is above the depicted level are hashed.

general, the direction of moisture flux anomalies (Fig. 9) is nearly the same as those in winds (Fig. 8). At 925 hPa, anomalous moisture is transported from the GoC into the NAM region, and distributed over a larger area at 850 hPa. At 700 hPa, a cyclonic moisture flux anomaly is centered in the northern GoC, with anomalous southerly moisture flux east of the GoC. The changes in moisture flux can be better visualized in the latitudinal vertical cross sections of meridional moisture flux across the NAM region shown in Fig. 10. Increased moisture flux within the channel-like GoC boundaries is seen at each of the cross sections, including the southern GoC and north into Arizona. In the middle levels, we note anomalous southerly moisture flux centered at 600 hPa east of the GoC, caused by the aforementioned lower midlevel geopotential heights in GoC\_WATER (Fig. 8). The southerly moisture flux increases in the GoC channel are an order of magnitude greater than the changes occurring in the middle levels, though the middle level changes occur over a much larger region. Thus, increased southerly moisture fluxes over the GoC and in the middle levels over the higher terrain are of similar total amounts.

Given these changes in moisture fluxes, it is no surprise that specific humidity increases in many areas. Over the GoC, increases in specific humidity extend from the GoC surface and up along the Sierra Madre Occidental directly east (right panels of Fig. 10). The middle levels directly over the GoC and west are drier in GoC\_WATER, due to the northerly moisture flux anomalies there as well as anomalous subsidence advecting drier air from above (Fig. 12; to be discussed). The increase in specific humidity also extends north of the GoC, once again most pronounced along the elevated topography.

Looking at the spatial pattern of change in specific humidity, we see rather widespread differences in moisture between GoC\_WATER and GoC\_LAND (Fig. 9). At 925 and 850 hPa, specific humidity increases in GoC\_WATER are most pronounced east and north of the GoC, in correspondence with

the cross sections in Fig. 10 (right panels). At 700 hPa, there is a rather clear pattern of increased specific humidity north and east of the GoC, and decreased specific humidity over and southwest of the GoC. However, the changes in specific humidity at this level cannot be entirely attributed to the changes in moisture fluxes at this level (at least with respect to the mean moisture flux anomalies). Although the anomalous southerly moisture flux northeast of the GoC is certainly favorable to increasing specific humidity over northwestern Mexico and Arizona/New Mexico, the increases in specific humidity extend north of the well-defined anomalous southerly moisture flux in GoC\_WATER. Here, it is likely the case that anomalous moisture is advected from the lower levels by the climatological NAM season ascent in this region. This would also explain why the northernmost specific humidity anomaly cross section in Fig. 10 follows the shape of the topography. Conversely, specific humidity anomalies over northwest Mexico may be less pronounced than over the SWUS due to strongly anomalous subsidence here (Fig. 12h). At 500 hPa, the main feature is negative specific humidity anomalies near and west of the GoC (Fig. 9).

#### d. Precipitation

Significant increases in precipitation in GoC\_WATER span over much of northern Mexico and the western United States, with a significant decrease in precipitation directly over the GoC (Fig. 11). Increases greater than 25% are simulated in parts of northwest Mexico and much of the SWUS, though large percentage increases west of Arizona/Utah reflect very small absolute increases (less than  $0.1 \text{ mm day}^{-1}$ ). Areas of increase in GoC\_WATER exceeding the 99% level of statistical significance ( $p < 0.01$  based on a  $t$  test) extend over most of north-central Mexico, Arizona, New Mexico, Utah, Colorado, southern Wyoming, and over much of the adjacent area extending northeastward toward the upper Great Lakes. A

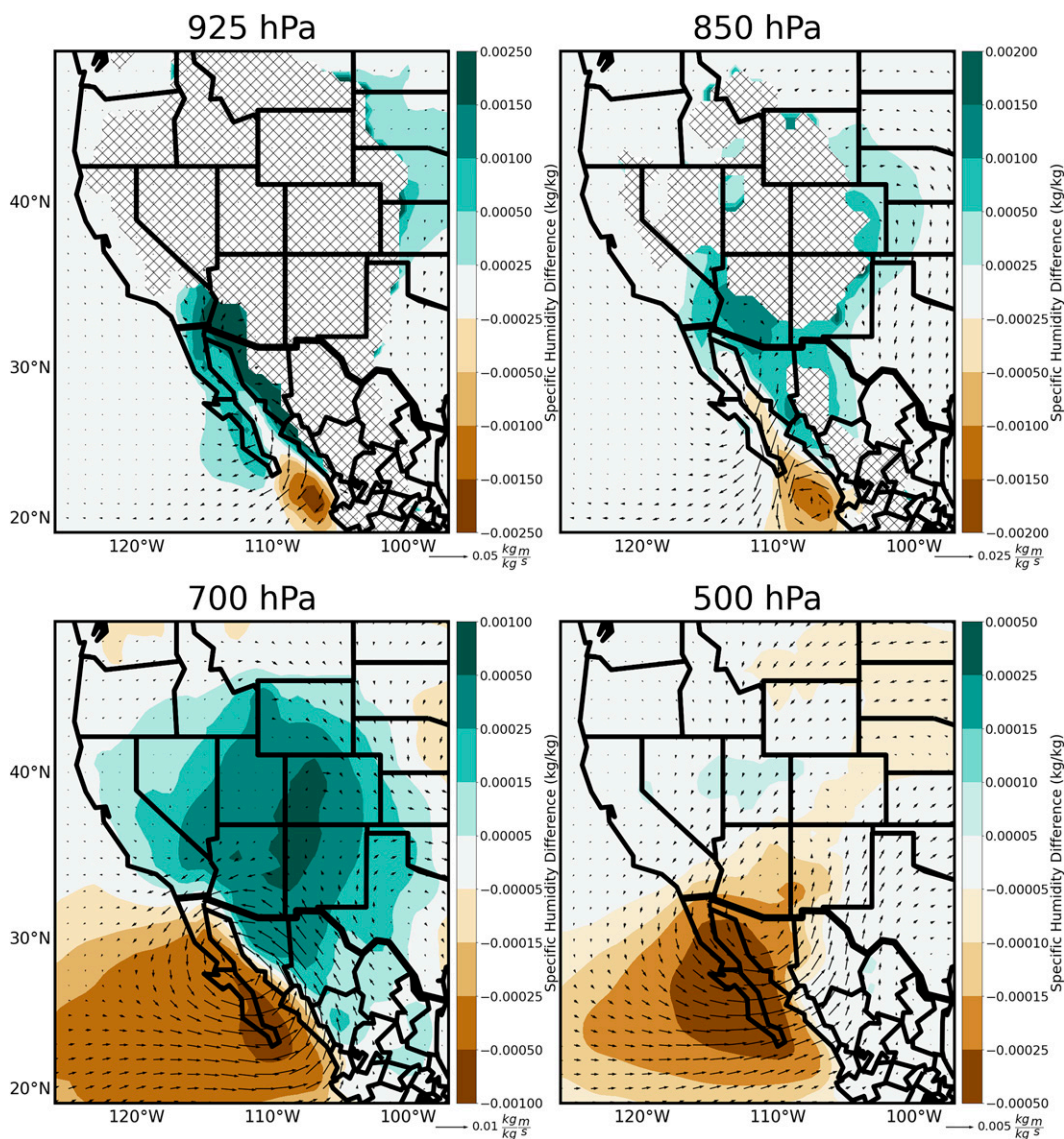


FIG. 9. July/August mean differences (GoC\_WATER – GoC\_LAND) for specific humidity (shading) and winds (vectors) at various pressure levels. Areas where the surface is above the depicted level are hashed.

particularly interesting result is the vast extent to which the GoC acts to increase precipitation. There will be a further analysis of factors likely responsible for the precipitation differences between the simulations after a discussion of land–atmosphere feedbacks in section 3e.

#### e. Land–atmosphere feedbacks

Significant land–atmosphere feedbacks occur in GoC\_WATER in response to widespread increases in precipitation. Higher precipitation in much of the western United States leads to lower surface air temperatures (Fig. 12a) via increased surface evaporation. This is because net radiation is only slightly higher in GoC\_WATER (not shown), and thus increased latent heat flux from the surface comes at the expense of sensible heat flux (Figs. 12b,d). Surface temperatures in

GoC\_WATER are 1°–2°C lower over a swath extending northeast of the GoC all the way to the central Great Plains of the United States, with temperatures 0.5°–1°C lower over an even larger area. In response to lower surface air temperatures, sea level pressure is higher over much of the central and western United States, in addition to the area of strongest increases directly over the GoC (Fig. 12c).

The effects of enhanced evaporative surface cooling in GoC\_WATER extend to the mid- to upper troposphere. Higher heights at 850 hPa are centered in the western United States (Fig. 13), corresponding to areas of higher sea level pressure. At 700 hPa, a relative high is centered over the far western United States. This is potentially a result of anomalous southerly flow on the west flank of anomalously high sea level pressure (i.e., warm air advection) and a lack of robust

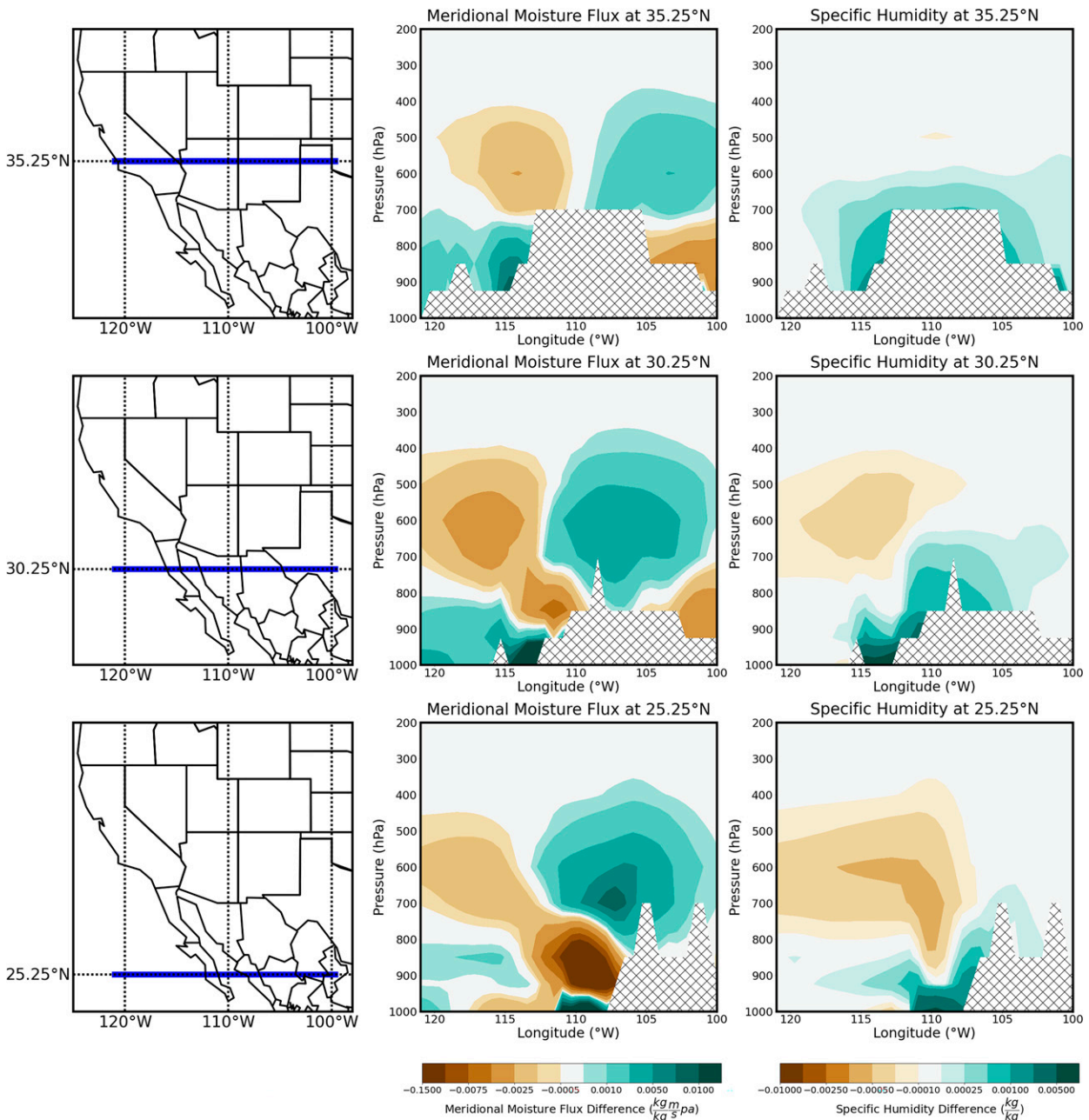


FIG. 10. July/August cross sections of mean differences (GoC\_WATER – GoC\_LAND) in (center) moisture fluxes and (right) specific humidity for (left) the latitudinal cross sections shaded in blue.

precipitation increase, which would likely otherwise cause evaporative surface cooling. In the Midwest United States, a 700-hPa low height anomaly is present, in addition to the aforementioned low 700-hPa height anomaly directly over the GoC. At 500 hPa, lower heights closely match the decreased lower-tropospheric temperatures in GoC\_WATER advected northeast by the southwest flow prevalent during the NAM season in SPEAR. The maximum height decreases at this level are displaced east due to the lack of sea level pressure increase farther east. Anomalous subsidence is also present

over much of northwestern Mexico, and extending north-northeast toward the northern U.S. Great Plains (Figs. 13g–i).

*f. Analysis of precipitation changes*

- 1) DECREASE IN PRECIPITATION OVER GoC;  
INCREASE EAST IN NORTHERN MEXICO

Over northern Mexico, there is a clear pattern of increased precipitation in the mainland of northwest Mexico and decreased precipitation over the GoC in GoC\_WATER

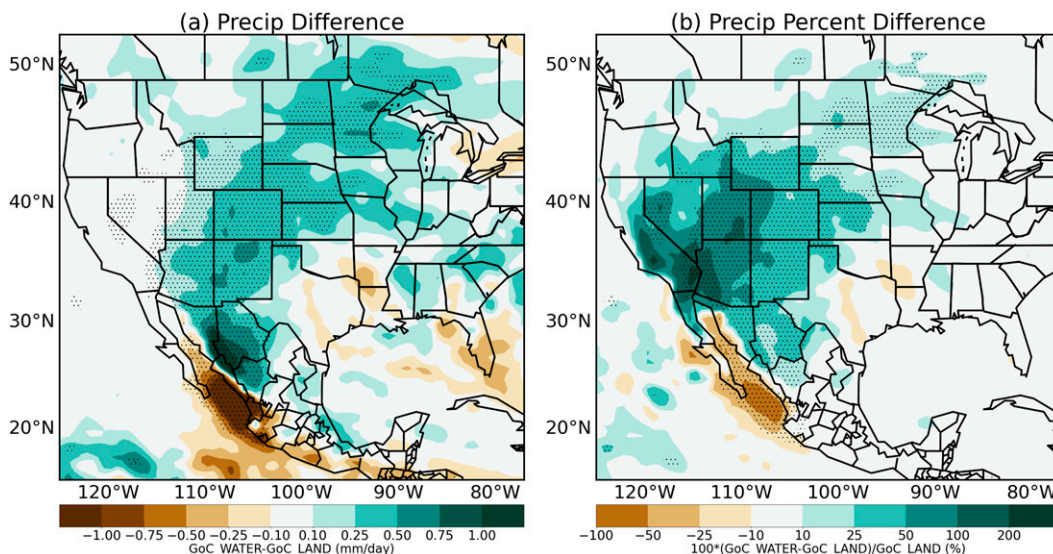


FIG. 11. July/August (a) precipitation differences ( $\text{GoC\_WATER} - \text{GoC\_LAND}$ ) and (b) percentage difference ( $\text{GoC\_WATER}$  vs  $\text{GoC\_LAND}$ ). Stippled areas are statistically significant at the 99% level ( $p < 0.01$ ).

(Fig. 11). Indeed, the largest increase (just east of the central GoC) and decrease (southeastern GoC) are separated only by a few hundred kilometers. This pattern of decrease over the GoC and increase northeast of the GoC is qualitatively similar to the steep drop in NAM climatological precipitation toward the GoC (Fig. 4). Interestingly, the decrease in precipitation occurs despite substantially higher CAPE over the GoC (Fig. 14), which results from sharply increased surface specific humidity (Fig. 10). In fact, CAPE is as much as  $3000 \text{ J kg}^{-1}$  greater in parts of the north-central GoC. The response of precipitation can be understood by looking at changes in convective inhibition (CIN), a measure of the energy needed to lift a parcel to the level at which it becomes positively buoyant with respect to the surrounding air. Even if high CAPE is present over the GoC, deep convection cannot occur if CIN is too high to be overcome. If CIN were unchanged between the two simulations, then the higher CAPE would likely translate to more precipitation. However, in this case it appears that the increase in CIN dominates. In other words, the increase in CIN in  $\text{GoC\_WATER}$  makes it more difficult to tap into CAPE, despite its substantial increase.

The sea-breeze circulation that arises in  $\text{GoC\_WATER}$  may also play a role in establishing the strong contrast between decreased precipitation over the GoC and increased precipitation over the Sierra Madre Occidental. In  $\text{GoC\_WATER}$ , strongly cooler surface temperatures (Fig. 7) lead to anomalous low-level subsidence (Fig. 12g). This anomalous sea-breeze circulation is also evidenced in the specific humidity difference cross sections shown in Fig. 10, where it is seen that increased specific humidity in  $\text{GoC\_WATER}$  is present near the surface over the GoC and extends to higher vertical levels along the adjacent shoreline. This is especially clear in the cross section at  $25.25^\circ\text{N}$  (southern GoC; bottom of Fig. 10). Here, there is a U-shaped pattern of increased specific humidity, with a decrease in specific humidity present as

low as 925 hPa directly over the GoC. There is observational evidence for a similar sea-breeze setup over the GoC both prior to and after the NAM onset. Fonseca-Hernandez et al. (2021), using rawinsonde observations from the 2004 North American monsoon experiment, show that a diurnal sea-breeze circulation sets up over the southern GoC, with subsidence over the GoC and ascent over the adjacent land.

The change in precipitation over the far southeast quadrant of the GoC (i.e., southeast over the southern tip of the Baja Peninsula) provides further evidence for the role of sea-breeze circulations. Here, CAPE is higher along with the rest of the GoC in  $\text{GoC\_WATER}$ , but CIN is actually lower, in contrast with the rest of the GoC. All else equal, an increase in CAPE and decrease in CIN would lead to an increase in precipitation. However, precipitation is strongly decreased here in  $\text{GoC\_WATER}$ . This area is unique in that a land-sea boundary is present in  $\text{GoC\_LAND}$  (Fig. 3). Upon the removal of land in  $\text{GoC\_WATER}$ , there is anomalous surface divergence here (Fig. 7a). The removal of both the thermal and frictional boundaries present in  $\text{GoC\_WATER}$  may be important. It is likely the case that the sea-breeze boundary present here in  $\text{GoC\_LAND}$  overcomes CIN via surface convergence and thus allows for greater precipitation than in  $\text{GoC\_WATER}$ .

## 2) INCREASE IN PRECIPITATION WEST OF U.S. CONTINENTAL DIVIDE

There is a large percentage increase in precipitation north of the GoC in  $\text{GoC\_WATER}$  (Fig. 11b), although the actual magnitude of increase is small farther west where July/August precipitation is low (Fig. 11a). In correspondence, specific humidity is increased near the surface and at 700 hPa (Fig. 9; left column). The pattern of specific humidity increases is similar to that of precipitation, but not exact (cf. Figs. 9, 11). Precipitation increases over the SWUS west of the Continental

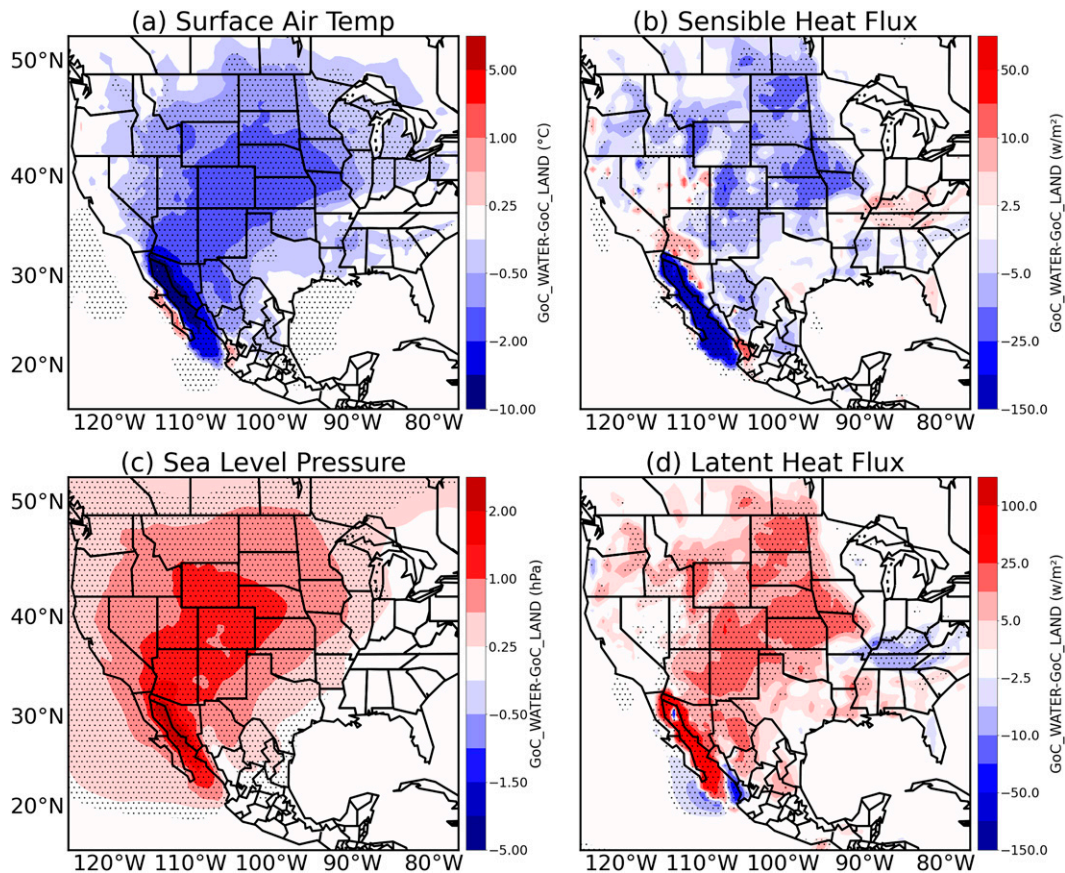


FIG. 12. July/August mean differences (GoC\_WATER – GoC\_LAND) in (a) surface air temperature, (b) surface sensible heat flux, (c) sea level pressure, and (d) latent heat flux. Stippled areas are statistically significant at the 99% level ( $p < 0.01$ ).

Divide scale well with the increase in CAPE. Here, mean July/August CAPE is increased by 25%–50% (Fig. 14), with higher values directly north of the GoC. Thus, increased low-level moisture in the SWUS appears to lead to disproportionately high precipitation increases via enhanced instability.

### 3) INCREASE IN PRECIPITATION EAST OF CONTINENTAL DIVIDE

Precipitation increases are also significant at the 99% level ( $p < 0.01$ ) over an expansive area east of the Continental Divide over north-central Mexico, New Mexico, Colorado, and they extend quite far east/northeast into the central United States (Fig. 11). Here, moisture in the lower levels cannot be advected directly from the GoC due to the blocking effect of topography. Additionally, the pattern of higher sea level pressure in the western United States (Fig. 12) is unfavorable for low-level moisture fluxes from the Gulf of Mexico into the central United States, as it leads to northerly surface flow anomalies over the Great Plains. It is important to note that a previous study shows SWUS summer evapotranspiration to contribute significantly to precipitation in the Great Plains (Dominguez et al. 2009), with the pattern of increases in GoC\_WATER somewhat consistent with areas where

moisture from the SWUS contributes to precipitation in the Great Plains. However, there are insignificant changes in moisture fluxes from the NAM region and specific humidity in the Great Plains in GoC\_WATER despite precipitation increases (Fig. 9). It is worth noting that in the real world, meso-scale convective systems are observed to initiate over the Rockies and propagate eastward toward the Great Plains into the nocturnal hours (Carbone et al. 2002). It could potentially be the case that precipitation systems over New Mexico and Colorado, increased in GoC\_WATER, propagate eastward into the Great Plains. However, the true cause for precipitation increases in the Great Plains is not entirely clear.

To better understand why precipitation increases in the Great Plains region, it is useful to average over the region and examine changes in moisture fluxes across the east–west and north–south boundaries. In Fig. 15, we analyze moisture fluxes in and out of the depicted Great Plains region and compare to precipitation and net precipitation. Here, we see that there is a slight decrease in net moisture flux into the region during July and a slight increase in August, with the July/August mean averaging out to near zero. This indicates that the increase in precipitation, when averaged across the region, is sourced from the recycling of surface evapotranspiration.

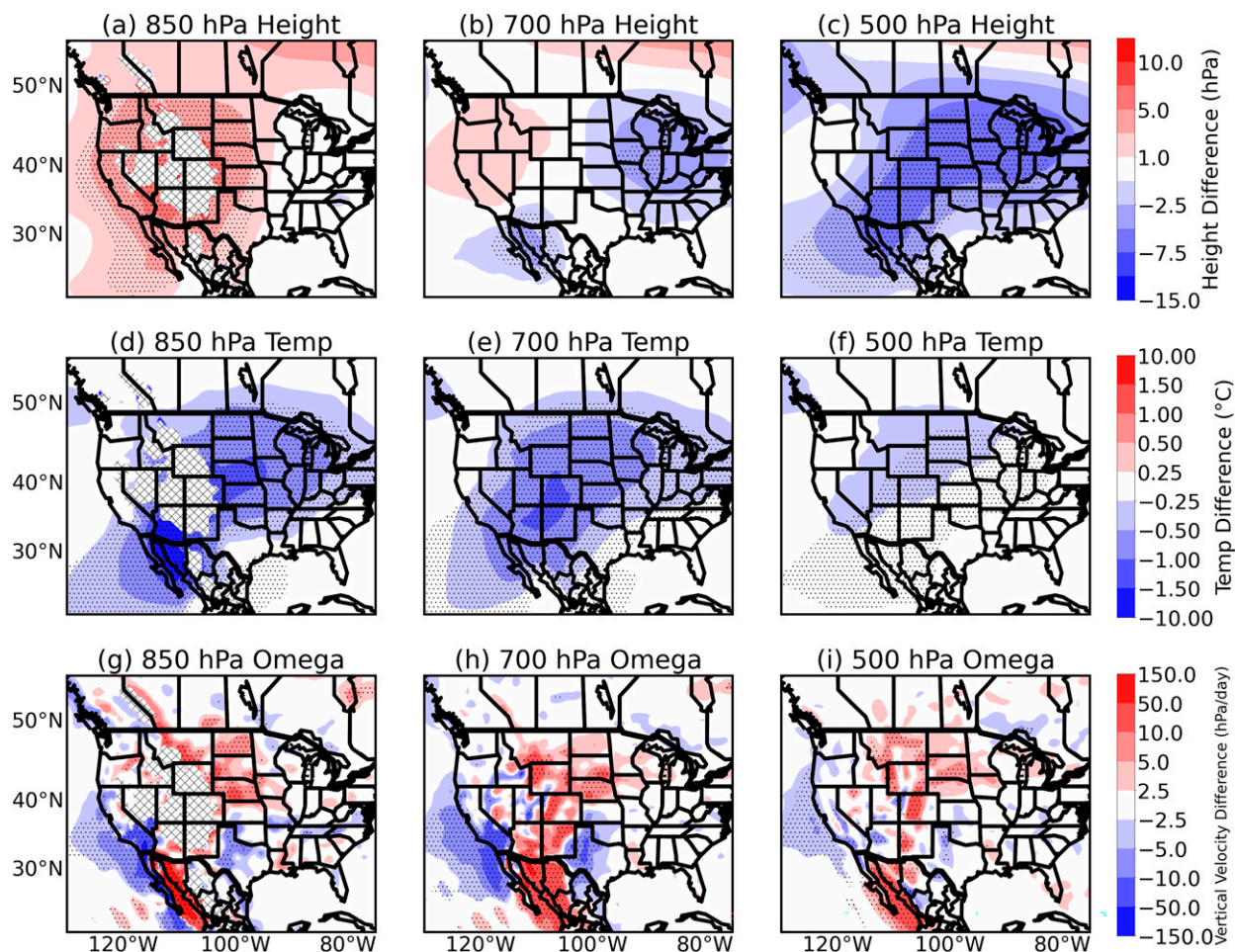


FIG. 13. July/August mean differences (GoC\_WATER – GoC\_LAND) at various pressure levels for (top) geopotential height, (middle) air temperature, and (bottom) vertical velocity. Stippled areas are statistically significant at the 99% level ( $p < 0.01$ ).

The increase in precipitation recycling may relate to higher soil moisture as a result of greater net precipitation during the months of May and June. However, it is also possible that precipitation would still be lower here in GoC\_LAND if soil moisture from the GoC\_WATER experiment were prescribed.

The precipitation increases during the months of May and June may relate to circulation changes. At 500 hPa, there is a large area of statistically significant (99% level) height decreases in GoC\_WATER stretching from northwest Mexico northeast into the west-central United States (Fig. 16). This may result from lower temperatures and higher sea level pressure in the SWUS and GoC, which likely results from a combination of the cool GoC surface and increased evapotranspiration over land due to higher precipitation in the months prior to then (Fig. 17; likely due simply to additional moisture supplied to synoptic weather systems by the GoC). Higher surface evaporation leads to cooler temperatures directly by decreasing sensible heat flux from the surface, while the higher sea level pressure in the SWUS acts to advect cooler air on the northeastern flank, where anomalous

northerly flow is present. It is not entirely obvious why precipitation here is sensitive to the presence of the GoC prior to (and during) the NAM season. Future work could investigate this in more detail.

#### 4. Discussion and summary

In this study, we explore the influence of the GoC in the NAM by comparing a simulation with a realistic GoC to one where the GoC is replaced with flat land. It is found that the GoC acts to directly alter the circulation in a way favorable to supplying moisture to the NAM region, inducing south-southeasterly flow along the GoC at the surface, and favoring cyclonic circulation at 700 hPa (Fig. 8b), which results in enhanced southerly flow of moisture into the NAM region at this level. In turn, precipitation is increased over much of northwestern Mexico, the SWUS, and central United States during July/August. Precipitation leads to land–atmosphere feedbacks via increased surface evaporation from higher soil moisture, which acts to resupply moisture, as well as lead to lower surface temperatures. In turn, sea level pressure is

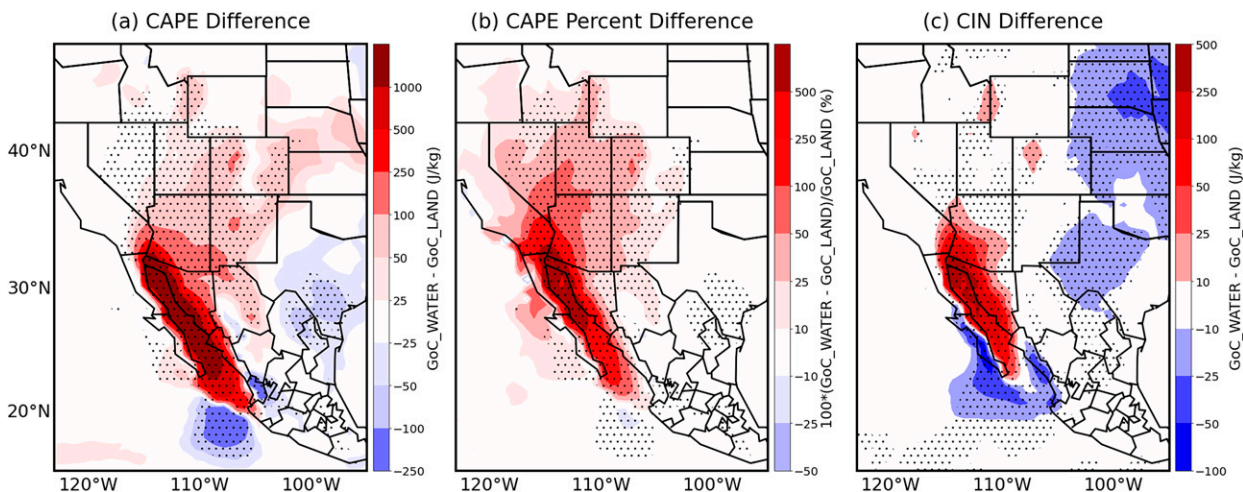


FIG. 14. July/August mean (a) CAPE difference, (b) CAPE percent difference, and (c) CIN difference. Stippled areas are significant at the 99% level ( $p < 0.01$ ).

increased over much of northwest Mexico and the west-central United States, with lower mid- to upper-tropospheric heights.

Changes in circulation between the simulations are particularly striking at the surface. In GoC\_LAND, westerly flow is present in the northern GoC, whereas south-southeasterly flow dominates in GoC\_WATER. As a result of this change in surface flow, along with substantially increased evaporation over the GoC, low-level moisture flux into the NAM region is increased in GoC\_WATER. The south-southeast surface flow that arises in GoC\_WATER results from both lower surface temperatures and lower surface friction. In GoC\_WATER, temperatures are 5°–10°C cooler over much of the GoC. This, in turn, leads to sea level pressure increases exceeding 2 hPa in some areas. Although the minimum sea

level pressure in the desert north of the GoC is lower in GoC\_LAND by 1–1.5 hPa, the gradient is more evenly distributed along the GoC, with a decreased west–east gradient in the northern GoC from the Pacific. The influence of surface friction is evidenced by a strengthening southerly component of winds in the southern GoC despite a reduced sea level pressure gradient there (Fig. 7). The breakdown between the effects of lower surface friction and lower surface temperatures could be further examined by comparing an additional simulation where the GoC is land, but surface friction is artificially lowered. More generally, the relative importance of direct changes in circulation versus GoC surface evaporation could be explored by comparing a modified GoC\_WATER simulation where GoC surface evaporation is suppressed.

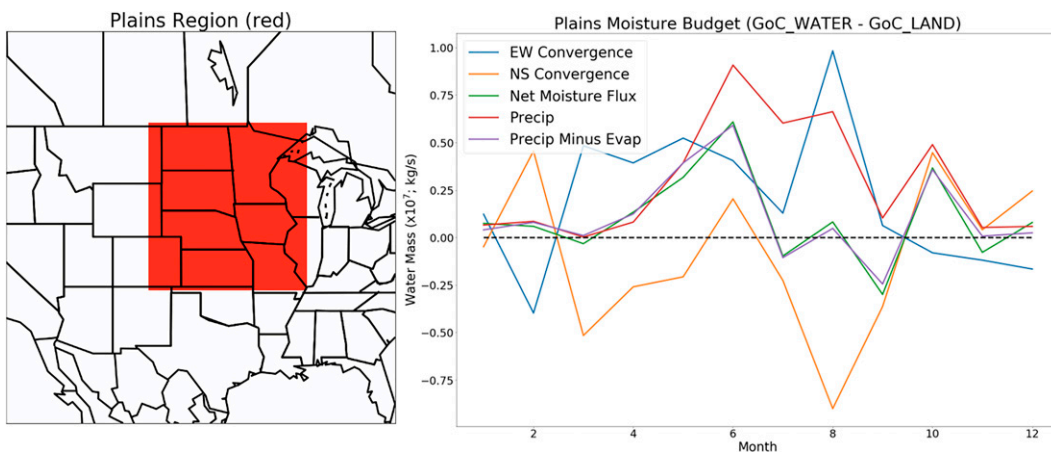


FIG. 15. (left) Moisture budget for the region in red. (right) Differences between simulations for each month (GoC\_WATER – GoC\_LAND). East–west moisture convergence (“EW Convergence”) is calculated as the total difference in moisture entering from the west and exiting the region through the eastern boundary. North–south moisture convergence (“NS Convergence”) is calculated as the total difference between moisture entering via the south boundary and exiting via the north boundary. Net moisture flux is defined as the total difference between moisture entering and exiting the region. Precipitation and precipitation minus evaporation are summed over the region.

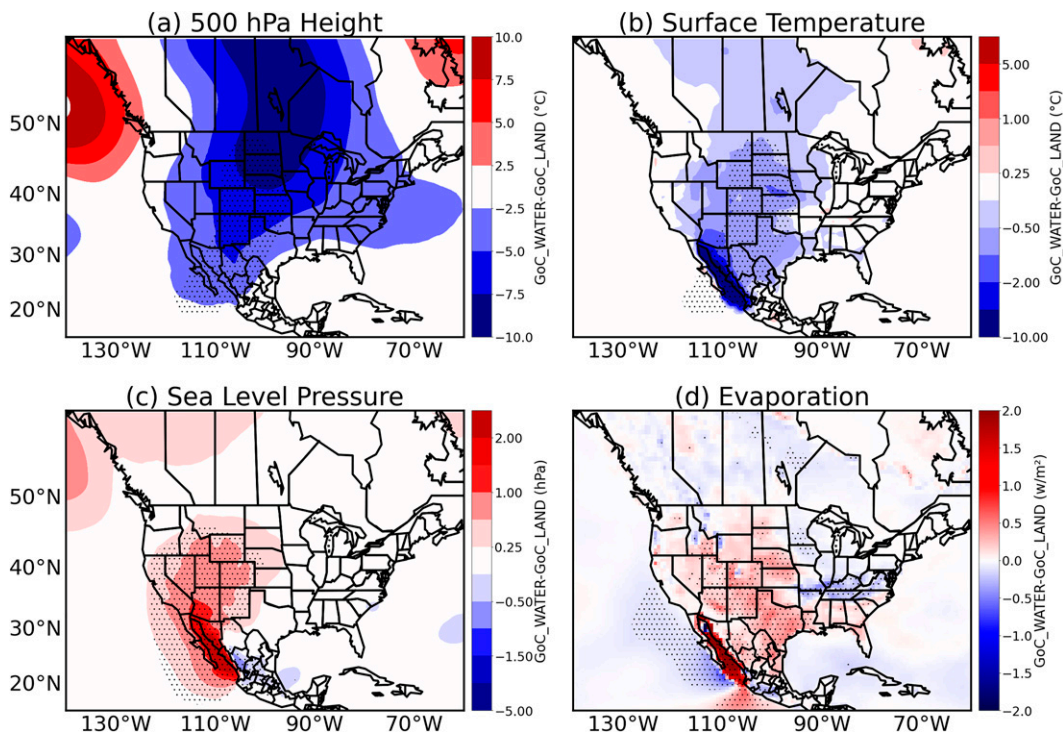


FIG. 16. May/June mean differences ( $\text{GoC\_WATER} - \text{GoC\_LAND}$ ) for various climate variables. Stippled areas are significant at the 99% level ( $p < 0.01$ ).

While previous studies, such as [Pascale et al. \(2016\)](#) and [Varuolo-Clarke et al. \(2019\)](#), emphasize the importance of the channel-like topography surrounding the GoC, our results show the GoC itself is an important feature. Our results do not, however, discount the role of the channel-like topography. For example, the southeasterly flow that arises in  $\text{GoC\_WATER}$  clearly flows within the topographic channel at the surface. Even above the GoC surface at 925 hPa, the flow is warped by the shape of channel-like topography ([Fig. 8](#)). If the Baja Peninsula were flattened in our experiments, it would likely be the case that the mean flow would have a westerly component over the GoC boundaries in both simulations,

which may inhibit NAM precipitation even in  $\text{GoC\_WATER}$ . Our results are also interesting in relation to work exploring the sensitivity of the NAM to GoC SSTs, such as the inability to simulate a realistic NAM with low GoC SSTs in [Stensrud et al. \(1995\)](#). As mentioned, [Erfani and Mitchell \(2014\)](#) suggest that cooler GoC SSTs strengthen the boundary layer inversion over its surface, confining moisture to a shallow layer near the surface. With higher SSTs, the moisture can extend deeper into the troposphere, and thus allow for more precipitation. Interestingly, in  $\text{GoC\_WATER}$ , there is a significantly stabilized temperature profile near the surface due to the much cooler GoC surface, yet precipitation is strongly

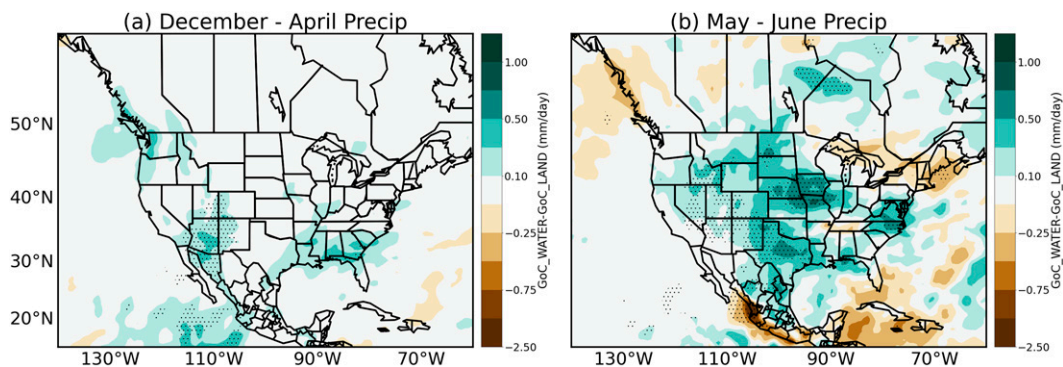


FIG. 17. (a) December–April and (b) May–June precipitation differences ( $\text{GoC\_WATER} - \text{GoC\_LAND}$ ). Stippled areas are significant at the 99% level ( $p < 0.01$ ).

increased over most of the NAM region. It may be the case that the GoC is warm enough that the moisture is not confined to a very thin layer, and not so warm that air from the cooler Pacific ventilates into the region (as is the case in GoC\_LAND). To better understand this relationship, it would be useful to perform further GoC\_WATER experiments with perturbed GoC SSTs.

The GoC has a large, widespread influence on precipitation over our simulations. Statistically significant increases in precipitation occur in GoC\_WATER over much of northwestern Mexico (immediately east of the GoC), the SWUS, and in much of the U.S. Great Plains region. Precipitation increases over northwestern Mexico exceed 25% in many areas, with increases of 50%–100% or more over much of the NAM region west of the Continental Divide in the SWUS. Farther east, increases of 25%–50% occur over much of New Mexico, Colorado, and Wyoming, with increases of 10%–25% over much of the Great Plains region. It should be noted that SPEAR has a NAM dry bias (Fig. 4), which may influence the sensitivity of the NAM to the presence of the GoC in our simulations. It is unclear whether the dry bias causes the GoC's influence on NAM precipitation to be overstated or understated in the model. While similar experiments performed with different climate models would be useful, the widespread increases in rainfall, along with robust circulation changes over the GoC, suggest the GoC is an important feature.

Attributing specifics to the relative importance of moisture flux changes at each level and land feedbacks in each location is a challenge. Directly north and east of the GoC, the increase in low-level moisture, in part due to enhanced south-southeasterly flow and high rates of surface evaporation over the GoC, plays a clear role in the precipitation increases: higher surface moisture leads to higher CAPE and thus higher precipitation. Additionally, it is important to note that the 700-hPa height anomaly over the GoC in GoC\_WATER is observed to coincide with heavy precipitation events in the NAM region (Ordoñez et al. 2019). This suggests that the GoC may play a role in establishing a midtropospheric circulation regime favorable to NAM precipitation.

It is most unclear why precipitation increases extend so far northeastward into the U.S. Great Plains. On the one hand, the increase in this region would seem logical given the widespread increase in northwestern Mexico and the SWUS: the Great Plains is along the climatological trajectory of column-integrated moisture fluxes from the NAM region. Dominguez et al. (2009) also shows SWUS evapotranspiration to contribute to summer precipitation as far as the Great Plains region of the United States. Additionally, summer thunderstorms are observed to form over the Rockies during the day and propagate eastward into the Great Plains toward the night (Carbone et al. 2002). However, there is not a clear increase in moisture flux toward the Great Plains from the NAM region in GoC\_WATER (Fig. 9). In the Plains region, the increase in precipitation may relate to higher soil moisture due to higher May/June precipitation. However, it is not fully clear why late spring precipitation is increased here, and whether a similar mechanism continues to have an influence during the NAM season. The apparent sensitivity of Great

Plains precipitation to the presence of the GoC in our simulations would be an interesting topic to further explore. For example, it may help us understand the Great Plains dry bias in SPEAR (Fig. 5). A further pair of simulations controlling land feedbacks (i.e., prescribing climatological soil moisture) could help further dissect why the GoC influences precipitation in this region.

Overall, our results suggest the GoC is a key component of the NAM system. The high sensitivity of the NAM to small-scale dynamics over the GoC should be taken into careful consideration in climate simulations. For one, the GoC is often poorly resolved in model experiments. Additionally, deficiencies in simulated dynamics over the GoC could help explain NAM model biases and potentially be a factor in the disparity between different NAM anthropogenic warming experiments.

*Acknowledgments.* Funding for this project is from the Cooperative Institute for Modeling the Earth System (CIMES), a collaboration between the Geophysical Fluid Dynamics Laboratory (GFDL) and Princeton University. We thank William F. Cooke and Sergey Malyshev for their help in preparing our simulations.

*Data availability statement.* Data are available upon request.

## REFERENCES

- Adams, D. K., and A. C. Comrie, 1997: The North American monsoon. *Bull. Amer. Meteor. Soc.*, **78**, 2197–2214, [https://doi.org/10.1175/1520-0477\(1997\)078<2197:TNAM>2.0.CO;2](https://doi.org/10.1175/1520-0477(1997)078<2197:TNAM>2.0.CO;2).
- , and E. P. Souza, 2009: CAPE and convective events in the Southwest during the North American monsoon. *Mon. Wea. Rev.*, **137**, 83–98, <http://doi.org/10.1175/2008MWR2502.1>.
- Barlow, M., S. Nigam, and E. H. Berbery, 1998: Evolution of the North American monsoon system. *J. Climate*, **11**, 2238–2257, [https://doi.org/10.1175/1520-0442\(1998\)011<2238:EOTNAM>2.0.CO;2](https://doi.org/10.1175/1520-0442(1998)011<2238:EOTNAM>2.0.CO;2).
- Becker, E. J., and E. H. Berbery, 2008: The diurnal cycle of precipitation over the North American monsoon region during the name 2004 field campaign. *J. Climate*, **21**, 771–787, <https://doi.org/10.1175/2007JCLI1642.1>.
- Boos, W. R., and Z. Kuang, 2010: Dominant control of the South Asian monsoon by orographic insulation versus plateau heating. *Nature*, **463**, 218–222, <https://doi.org/10.1038/nature08707>.
- , and S. Pascale, 2021: Mechanical forcing of the North American monsoon by orography. *Nature*, **599**, 611–615, <https://doi.org/10.1038/s41586-021-03978-2>.
- Bordoni, S., P. E. Ciesielski, R. H. Johnson, B. D. McNoldy, and B. Stevens, 2004: The low-level circulation of the North American monsoon as revealed by QuikSCAT. *Geophys. Res. Lett.*, **31**, L10109, <https://doi.org/10.1029/2004GL020009>.
- Brenner, I. S., 1973: A surge of maritime tropical air—Gulf of California to the southwestern United States. NOAA Tech. Memo. NWS WR88, 47 pp., [https://www.weather.gov/media/wrh/online\\_publications/TMs/TM-88.pdf](https://www.weather.gov/media/wrh/online_publications/TMs/TM-88.pdf).
- Carbone, R. E., J. D. Tuttle, D. A. Ahijevych, and S. B. Trier, 2002: Inferences of predictability associated with warm season precipitation episodes. *J. Atmos. Sci.*, **59**, 2033–2056,

- [https://doi.org/10.1175/1520-0469\(2002\)059<2033:IOPAWW>2.0.CO;2](https://doi.org/10.1175/1520-0469(2002)059<2033:IOPAWW>2.0.CO;2).
- Carleton, A. M., D. A. Carpenter, and P. J. Weser, 1990: Mechanisms of interannual variability of the Southwest United States summer rainfall maximum. *J. Climate*, **3**, 999–1015, [https://doi.org/10.1175/1520-0442\(1990\)003<0999:MOIVOT>2.0.CO;2](https://doi.org/10.1175/1520-0442(1990)003<0999:MOIVOT>2.0.CO;2).
- Castro, C. L., H.-I. Chang, F. Dominguez, C. Carrillo, J.-K. Schemm, and H.-M. Henry Juang, 2012: Can a regional climate model improve the ability to forecast the North American monsoon? *J. Climate*, **25**, 8212–8237, <https://doi.org/10.1175/JCLI-D-11-00441.1>.
- Cook, B. I., and R. Seager, 2013: The response of the North American monsoon to increased greenhouse gas forcing. *J. Geophys. Res. Atmos.*, **118**, 1690–1699, <https://doi.org/10.1002/jgrd.50111>.
- Delworth, T. L., and Coauthors, 2020: Spear: The next generation GFDL modeling system for seasonal to multidecadal prediction and projection. *J. Adv. Model. Earth Syst.*, **12**, e2019MS001895, <https://doi.org/10.1029/2019MS001895>.
- Dominguez, F., J. C. Villegas, and D. D. Breshears, 2009: Spatial extent of the North American monsoon: Increased cross-regional linkages via atmospheric pathways. *Geophys. Res. Lett.*, **36**, L0740, <https://doi.org/10.1029/2008GL037012>.
- , G. Miguez-Macho, and H. Hu, 2016: WRF with water vapor tracers: A study of moisture sources for the North American monsoon. *J. Hydrometeor.*, **17**, 1915–1927, <https://doi.org/10.1175/JHM-D-15-0221.1>.
- Douglas, M. W., 1995: The summertime low-level jet over the Gulf of California. *Mon. Wea. Rev.*, **123**, 2334–2347, [https://doi.org/10.1175/1520-0493\(1995\)123<2334:TSLLJO>2.0.CO;2](https://doi.org/10.1175/1520-0493(1995)123<2334:TSLLJO>2.0.CO;2).
- , R. A. Maddox, K. Howard, and S. Reyes, 1993: The Mexican monsoon. *J. Climate*, **6**, 1665–1677, [https://doi.org/10.1175/1520-0442\(1993\)006<1665:TMM>2.0.CO;2](https://doi.org/10.1175/1520-0442(1993)006<1665:TMM>2.0.CO;2).
- Erfani, E., and D. Mitchell, 2014: A partial mechanistic understanding of the North American monsoon. *J. Geophys. Res. Atmos.*, **119**, 13 096–13 115, <https://doi.org/10.1002/2014JD022038>.
- Fonseca-Hernandez, M., C. Turrent, Y. G. Mayor, and I. Tereshchenko, 2021: Using observational and reanalysis data to explore the southern Gulf of California boundary layer during the North American monsoon onset. *J. Geophys. Res. Atmos.*, **126**, e2020JD033508, <https://doi.org/10.1029/2020JD033508>.
- Gadgil, S., 2018: The monsoon system: Land–sea breeze or the ITCZ? *J. Earth Syst. Sci.*, **127**, 1, <https://doi.org/10.1007/s12040-017-0916-x>.
- Geil, K. L., Y. L. Serra, and X. Zeng, 2013: Assessment of CMIP5 model simulations of the North American monsoon system. *J. Climate*, **26**, 8787–8801, <https://doi.org/10.1175/JCLI-D-13-00044.1>.
- Hales, J. E., Jr., 1972: Surges of maritime tropical air northward over the Gulf of California. *Mon. Wea. Rev.*, **100**, 298–306, [https://doi.org/10.1175/1520-0493\(1972\)100<0298:SOMTAN>2.3.CO;2](https://doi.org/10.1175/1520-0493(1972)100<0298:SOMTAN>2.3.CO;2).
- Held, I. M., and Coauthors, 2019: Structure and performance of GFDL's CM4.0 climate model. *J. Adv. Model. Earth Syst.*, **11**, 3691–3727, <https://doi.org/10.1029/2019MS001829>.
- Hersbach, H., and Coauthors, 2020: The ERA5 global reanalysis. *Quart. J. Roy. Meteor. Soc.*, **146**, 1999–2049, <https://doi.org/10.1002/qj.3803>.
- Higgins, R. W., Y. Yao, and X. L. Wang, 1997: Influence of the North American monsoon system on the U.S. summer precipitation regime. *J. Climate*, **10**, 2600–2622, [https://doi.org/10.1175/1520-0442\(1997\)010<2600:IOTNAM>2.0.CO;2](https://doi.org/10.1175/1520-0442(1997)010<2600:IOTNAM>2.0.CO;2).
- , Y. Chen, and A. V. Douglas, 1999: Interannual variability of the North American warm season precipitation regime. *J. Climate*, **12**, 653–680, [https://doi.org/10.1175/1520-0442\(1999\)012<0653:IVOTNA>2.0.CO;2](https://doi.org/10.1175/1520-0442(1999)012<0653:IVOTNA>2.0.CO;2).
- Hsu, P.-C., T. Li, J.-J. Luo, H. Murakami, A. Kitoh, and M. Zhao, 2012: Increase of global monsoon area and precipitation under global warming: A robust signal? *Geophys. Res. Lett.*, **39**, L06701, <https://doi.org/10.1029/2012GL051037>.
- Jana, S., B. Rajagopalan, M. A. Alexander, and A. J. Ray, 2018: Understanding the dominant sources and tracks of moisture for summer rainfall in the southwest United States. *J. Geophys. Res. Atmos.*, **123**, 4850–4870, <https://doi.org/10.1029/2017JD027652>.
- Japan Meteorological Agency, 2013: JRA-55: Japanese 55-year reanalysis, daily 3-hourly and 6-hourly data. Research Data Archive at the National Center for Atmospheric Research, <https://doi.org/10.5065/D6HH6H41>.
- Kim, J., J. Kim, J. D. Farrara, and J. O. Roads, 2005: The effects of the Gulf of California SSTs on warm-season rainfall in the southwestern United States and northwestern Mexico: A regional model study. *J. Climate*, **18**, 4970–4992, <https://doi.org/10.1175/JCLI3584.1>.
- Kitoh, A., H. Endo, K. Krishna Kumar, I. F. A. Cavalcanti, P. Goswami, and T. Zhou, 2013: Monsoons in a changing world: A regional perspective in a global context. *J. Geophys. Res. Atmos.*, **118**, 3053–3065, <https://doi.org/10.1002/jgrd.50258>.
- Lee, J.-Y., and B. Wang, 2014: Future change of global monsoon in the CMIP5. *Climate Dyn.*, **42**, 101–119, <https://doi.org/10.1007/s00382-012-1564-0>.
- Liang, X.-Z., J. Zhu, K. E. Kunkel, M. Ting, and J. X. Wang, 2008: Do CGCMs simulate the North American monsoon precipitation seasonal–interannual variability? *J. Climate*, **21**, 4424–4448, <https://doi.org/10.1175/2008JCLI2174.1>.
- Lock, A. P., A. R. Brown, M. R. Bush, G. M. Martin, and R. N. B. Smith, 2000: A new boundary layer mixing scheme. Part I: Scheme description and single-column model tests. *Mon. Wea. Rev.*, **128**, 3187–3199, [https://doi.org/10.1175/1520-0493\(2000\)128<3187:ANBLMS>2.0.CO;2](https://doi.org/10.1175/1520-0493(2000)128<3187:ANBLMS>2.0.CO;2).
- Meyer, J. D. D., and J. Jin, 2017: The response of future projections of the North American monsoon when combining dynamical downscaling and bias correction of CCSM4 output. *Climate Dyn.*, **49**, 433–447, <https://doi.org/10.1007/s00382-016-3352-8>.
- Mitchell, D. L., D. Ivanova, R. Rabin, T. J. Brown, and K. Redmond, 2002: Gulf of California Sea surface temperatures and the North American monsoon: Mechanistic implications from observations. *J. Climate*, **15**, 2261–2281, [https://doi.org/10.1175/1520-0442\(2002\)015<2261:GOCSST>2.0.CO;2](https://doi.org/10.1175/1520-0442(2002)015<2261:GOCSST>2.0.CO;2).
- Mo, K. C., and H. H. Juang, 2003: Influence of sea surface temperature anomalies in the Gulf of California on North American monsoon rainfall. *J. Geophys. Res.*, **108**, 4112, <https://doi.org/10.1029/2002JD002403>.
- Ordoñez, P., R. Nieto, L. Gimeno, P. Ribera, D. Gallego, C. A. Ochoa-Moya, and A. I. Quintanar, 2019: Climatological moisture sources for the western North American monsoon through a Lagrangian approach: Their influence on precipitation intensity. *Earth Syst. Dyn.*, **10**, 59–72, <https://doi.org/10.5194/esd-10-59-2019>.
- Pascale, S., S. Bordoni, S. B. Kapnick, G. A. Vecchi, L. Jia, T. L. Delworth, S. Underwood, and W. Anderson, 2016: The impact of horizontal resolution on North American monsoon

- Gulf of California moisture surges in a suite of coupled global climate models. *J. Climate*, **29**, 7911–7936, <https://doi.org/10.1175/JCLI-D-16-0199.1>.
- , W. R. Boos, S. Bordoni, T. L. Delworth, S. B. Kapnick, H. Murakami, G. A. Vecchi, and W. Zhang, 2017: Weakening of the North American monsoon with global warming. *Nat. Climate Change*, **7**, 806–812, <https://doi.org/10.1038/nclimate3412>.
- Rayner, N. A., D. E. Parker, E. B. Horton, C. K. Folland, L. V. Alexander, D. P. Rowell, E. C. Kent, and A. Kaplan, 2003: Global analyses of sea surface temperature, sea ice, and night marine air temperature since the late nineteenth century. *J. Geophys. Res.*, **108**, 4407, <https://doi.org/10.1029/2002JD002670>.
- Rowson, D. R., and S. J. Colucci, 1992: Synoptic climatology of thermal low-pressure systems over south-western North America. *Int. J. Climatol.*, **12**, 529–545, <https://doi.org/10.1002/joc.3370120602>.
- Schiffer, N. J., and S. W. Nesbitt, 2012: Flow, moisture, and thermodynamic variability associated with Gulf of California surges within the North American monsoon. *J. Climate*, **25**, 4220–4241, <https://doi.org/10.1175/JCLI-D-11-00266.1>.
- Schneider, U., A. Becker, P. Finger, A. Meyer-Christoffer, B. Rudolf, and M. Ziese, 2011: GPCC full data reanalysis version 6.0 at 0.5: Monthly land-surface precipitation from rain-gauges built on GTS-based and historic data. Research Data Archive at the National Center for Atmospheric Research, [https://doi.org/10.5676/dwd\\_gpcc/fd\\_m\\_v6\\_050](https://doi.org/10.5676/dwd_gpcc/fd_m_v6_050).
- Stensrud, D. J., R. L. Gall, S. L. Mullen, and K. W. Howard, 1995: Model climatology of the Mexican monsoon. *J. Climate*, **8**, 1775–1794, [https://doi.org/10.1175/1520-0442\(1995\)008<1775:MCOTMM>2.0.CO;2](https://doi.org/10.1175/1520-0442(1995)008<1775:MCOTMM>2.0.CO;2).
- Tang, M., and E. R. Reiter, 1984: Plateau monsoons of the Northern Hemisphere: A comparison between North America and Tibet. *Mon. Wea. Rev.*, **112**, 617–637, [https://doi.org/10.1175/1520-0493\(1984\)112<0617:PMOTNH>2.0.CO;2](https://doi.org/10.1175/1520-0493(1984)112<0617:PMOTNH>2.0.CO;2).
- Turrent, C., and T. Cavazos, 2009: Role of the land-sea thermal contrast in the interannual modulation of the North American monsoon. *Geophys. Res. Lett.*, **36**, L02808, <https://doi.org/10.1029/2008GL036299>.
- Varuolo-Clarke, A. M., K. A. Reed, and B. Medeiros, 2019: Characterizing the North American monsoon in the Community Atmosphere Model: Sensitivity to resolution and topography. *J. Climate*, **32**, 8355–8372, <https://doi.org/10.1175/JCLI-D-18-0567.1>.
- Zehnder, J. A., 2004: Dynamic mechanisms of the gulf surge. *J. Geophys. Res.*, **109**, D10107, <https://doi.org/10.1029/2004JD004616>.
- Zhao, M., and Coauthors, 2018: The GFDL global atmosphere and land model AM4.0/LM4.0: 2. Model description, sensitivity studies, and tuning strategies. *J. Adv. Model. Earth Syst.*, **10**, 735–769, <https://doi.org/10.1002/2017MS001209>.
- Zhu, J., and X.-Z. Liang, 2013: Impacts of the Bermuda high on regional climate and ozone over the United States. *J. Climate*, **26**, 1018–1032, <https://doi.org/10.1175/JCLI-D-12-00168.1>.